

Global Permutation Entropy

Abhijeet Avhale¹, Joscha Diehl¹, Niraj Velankar¹, and Emanuele Verri¹

¹Institute of Mathematics and Computer Science, University of Greifswald, 17489 Greifswald, Germany

August 28, 2025

Permutation Entropy, introduced by Bandt and Pompe, is a widely used complexity measure for real-valued time series that is based on the relative order of values within *consecutive* segments of fixed length. After standardizing each segment to a permutation and computing the frequency distribution of these permutations, Shannon Entropy is then applied to quantify the series' complexity.

We introduce Global Permutation Entropy (GPE), a novel index that considers *all* possible patterns of a given length, including non-consecutive ones. Its computation relies on recently developed algorithms that enable the efficient extraction of full permutation profiles. We illustrate some properties of GPE and demonstrate its effectiveness through experiments on synthetic datasets, showing that it reveals structural information not accessible through standard permutation entropy. We provide a Julia package for the calculation of GPE at <https://github.com/AThreeH1/Global-Permutation-Entropy>.

Contents

1	Introduction	1
1.1	Our Contributions	2
2	Global Permutation Entropy	3
2.1	Fast Computation of the 2-,3-,4-,5-,6-Profiles	4
3	Experiments	5
3.1	Window size and convergence	6
3.2	Noise Detection	7
3.3	Periodic signal with additive noise which increases linearly over time	9
4	Conclusion and Outlook	10

1 Introduction

Permutation Entropy (PE), introduced by Bandt and Pompe in [BP02], is a simple and widely used method for quantifying the complexity of time series. Given a time series, classical PE analyzes ordinal patterns extracted from short consecutive segments of the time series by ranking their values and counting the frequencies of the resulting permutations. The Shannon

entropy of this empirical distribution then quantifies the diversity of these ordinal patterns: higher entropy reflects greater randomness or complexity in the data.

The computational cost of PE scales linearly with the length of the time series, $\mathcal{O}(n)$, making it applicable even to large datasets. Moreover, since PE depends solely on the relative ordering of values, it is invariant under monotonic transformations and robust to observational noise. Often, a delay parameter τ is introduced ([KL03]) to sample points within the time series at specific time steps, enabling the capture of slower dynamics or multi-scale structures. PE has been successfully applied to data in various fields, including finance [ZSW13], neuroscience [Fer+14; LOR07], and machine learning [Liu+22].

Since classical permutation entropy restricts attention to patterns formed from consecutive or regularly spaced points, it potentially overlooks more intricate dependencies, especially in short or structured signals. We therefore propose **Global Permutation Entropy** (GPE), whose computation is based on *all* strictly increasing index combinations of size k drawn from the full time series $(X_t)_{t=1}^n$. In other words, GPE requires the full *permutation profile* of order k , which records the frequency of each permutation of size k across all $\binom{n}{k}$ increasing subsets of the index set. Naively, this has a computational cost of $\mathcal{O}(n^k)$, which becomes prohibitive for large n . However, recent algorithmic breakthroughs have led to efficient methods for counting permutation patterns, with complexities that scale at most quadratically¹ in n for all orders up to $k = 7$ [BL24; DV24; EL21]. See Section 2.1 for details. As a result, computing the GPE for orders up to 7 is now computationally feasible, even for large input sizes.

1.1 Our Contributions

- We propose *Global Permutation Entropy* (GPE), a new complexity measure that is conceptually simple but whose naive calculation is computationally intractable for even moderate window sizes and orders. Only recent advances in permutation pattern counting have made its practical implementation viable.
- We provide a Julia library (<https://github.com/AThreeH1/Global-Permutation-Entropy>) for computing global permutation entropy up to order 6, using corner trees [EL21] and their generalizations [BL24; DV24] to count global permutation patterns. In particular, we include fast implementations for the 3-, 4-, 5-, and 6-permutation pattern profiles.
- We test the library on synthetic data to tease out differences between GPE and PE.
- Despite its higher computational cost compared to classical PE, GPE offers several desirable properties:
 - For completely random signals and fixed order $k > 2$, $\text{GPE}(k)$ converges faster than $\text{PE}(k)$ to the “correct” value of 1. See Section 3.1.
 - In certain scenarios involving a noisy periodic signal with a sudden increase in noise level, GPE detects changes more quickly than PE. See Section 3.2.
 - When noise is gradually added to a periodic signal, GPE remains highly descriptive and robust across different orders and window sizes. Its performance is also comparable to PE when the latter is carefully tuned (e.g., by using optimal delays or averaging across delays). See Section 3.3.

¹modulo a polylogarithmic factor.

2 Global Permutation Entropy

Let $(X_t)_{t=1}^n$ be a real-valued time series of length n . For each strictly increasing index tuple (i_1, i_2, \dots, i_k) with $1 \leq i_1 < i_2 < \dots < i_k \leq n$, we extract the subsequence $(X_{i_1}, X_{i_2}, \dots, X_{i_k})$ and rank its values from smallest to largest. This ranking² defines a unique permutation $\sigma \in S_k$, where $\sigma(j) = r$ means that the element in position j of the subsequence is the r -th smallest among the k elements. We denote the collection of all strictly increasing index tuples of size k by

$$\mathcal{I}_k := \{(i_1, i_2, \dots, i_k) \mid 1 \leq i_1 < i_2 < \dots < i_k \leq n\}.$$

The relative frequency of each ordinal pattern $\sigma \in S_k$ is then given by

$$p(\sigma) := \frac{\#\{(i_1, \dots, i_k) \in \mathcal{I}_k : (X_{i_1}, \dots, X_{i_k}) \text{ has permutation type } \sigma\}}{\binom{n}{k}}. \quad (1)$$

The (raw) **Global Permutation Entropy** (GPE) of order k is defined as the Shannon entropy of this empirical distribution:

$$\widehat{\text{GPE}}(k) := - \sum_{\sigma \in S_k} p(\sigma) \log p(\sigma),$$

with the convention $0 \log 0 := 0$.

For completeness, recall that the (raw) **Permutation Entropy** (PE) of order k with delay τ is defined as

$$\begin{aligned} \widehat{\text{PE}}(k; \tau) &:= - \sum_{\sigma \in S_k} q(\sigma) \log q(\sigma), \\ q(\sigma) &:= \frac{\#\{1 \leq i \leq n - \tau(k-1) : (X_i, X_{i+\tau}, \dots, X_{i+\tau(k-1)}) \text{ has permutation type } \sigma\}}{n - \tau(k-1)}. \end{aligned}$$

Observe that

- For any order k , both $\widehat{\text{GPE}}(k)$ and $\widehat{\text{PE}}(k; \tau)$ take values in the interval $[0, \log(k!)]$. The lower bound is attained when only a single pattern occurs, namely either the identity (increasing) or the reverse (descending) permutation, as in monotone signals, while the upper bound is reached when all $k!$ patterns are equally likely (as in purely random signals).
- Both GPE and PE depend only on the relative ordering of the values. They are therefore *invariant under monotone transformations* of the time series and *robust to observational noise*.

In what follows, we shall work with the normalized versions of both quantities:

$$\text{GPE}(k) := \frac{\widehat{\text{GPE}}(k)}{\log(k!)}, \quad \text{PE}(k, \tau) := \frac{\widehat{\text{PE}}(k; \tau)}{\log(k!)}$$

When the default delay $\tau = 1$ is used, we simply write $\widehat{\text{PE}}(k) := \widehat{\text{PE}}(k; 1)$ and $\text{PE}(k) := \widehat{\text{PE}}(k) / \log(k!)$.

As an example, Figure 1 illustrates the 3-profile of the permutation $[7 \ 4 \ 3 \ 5 \ 2 \ 1 \ 6]$ used to compute $\text{GPE}(3)$, along with the frequencies of the 3 patterns used to compute $\text{PE}(3; 1)$ and $\text{PE}(3; 2)$ respectively. For the rest of the paper, we will stick to the convention that GPE (and related quantities) will always be depicted in red, and PE (and related quantities) in blue.

²In case a tie occurs, values are ordered according to their time of appearance.

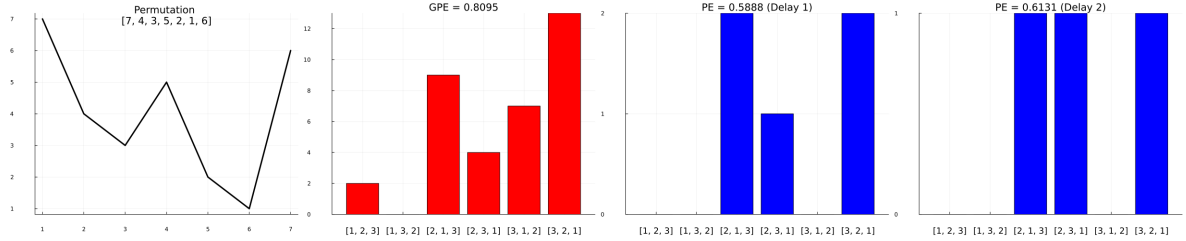


Figure 1: Example illustrating the 3-profile and pattern frequencies used to compute $\text{GPE}(3)$, $\text{PE}(3; 1)$ and $\text{PE}(3; 2)$ respectively.

In Figure 2, on the left, we show the realization of a signal which consists of a straight line (with slope equal to 0.05) from which points 1 up to 40 are considered. At each time point, the added noise follows a normal distribution $\mathcal{N}(0, 0.025)$. On the right, we depict the sinus function on 40 equispaced points between 0 and π . Again, at each time point, we add a realization from $\mathcal{N}(0, 0.025)$.

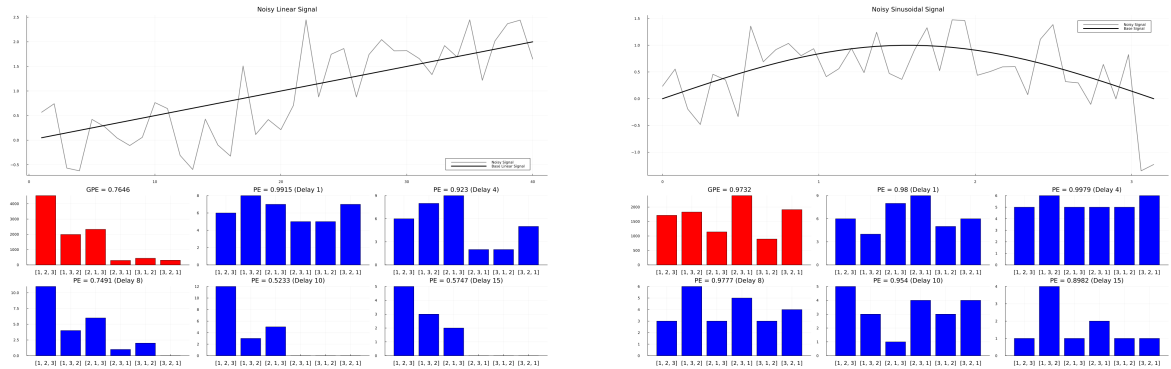


Figure 2: Left: increasing straight line with noise. Right: Sinus function from 0 to π with noise.

2.1 Fast Computation of the 2-,3-,4-,5-,6-Profiles

In the seminal work [EL21], it was realized that (certain) permutation patterns can be counted by counting combinatorial structures called *corner trees*. The tree structure of the latter leads to a fast algorithm for counting their occurrences in a time series.

In order 2 and 3, *all* permutation patterns can be counted using corner trees, and the corresponding algorithm runs in time $\mathcal{O}(n \log n)$. For higher orders, additional patterns need to be counted. Some have already been proposed in [EL21], with slight extensions in [DV24]. Finally, with the work of [BL24], all patterns up to order 5 can be counted in (almost) subquadratic time, while all patterns up to order 7 can be counted in (almost) quadratic time.

The **permutation profile** of order k for a time series of length n is the collection of counts of all permutation patterns of order k appearing in the time series. See Figure 1 for the 3-profile for a time series of length 7. We remark that when using the methods described above to compute the permutation profile of order k one necessarily computes the profiles for all orders $i \leq k$ as well.

Profile Implementations In our repository [Avh+25], the profiles of order $k = 2, \dots, 6$ are implemented. For details regarding the implementation and time-complexity of the algorithms, we refer to [BL24; EL21; DV24]. We summarize them below:

- **2-profile:** Implemented using two *corner trees*, each with two vertices. Corner trees were

introduced in [EL21]. Counting the occurrences of these trees requires $\mathcal{O}(n \log n)$ time, so the entire profile can be computed in $\mathcal{O}(n \log n)$ time.

- **3-profile:** Builds on the two-vertex corner trees from the 2-profile by adding six corner trees with three vertices. They span the full 3-profile and hence, the total computation time remains $\mathcal{O}(n \log n)$.
- **4-profile:** Extends the previous profiles by incorporating 23 additional corner trees with four vertices and the permutation pattern [3 2 1 4], which is counted in $\mathcal{O}(n^{5/3} \log^2 n)$ time using the algorithm from [EL21]. Thus, the entire 4-profile can be computed in $\mathcal{O}(n^{5/3} \log^2 n)$ time.
- **5-profile:** Extends the 4-profile with 100 corner trees, 10 tree double posets from the $\text{Tree}_{5/3}$ family (introduced in [DV24]) together with their images under nontrivial D_4 actions, all with five vertices. The remaining 10 double posets are obtained using *marked patterns* (introduced in [BL24]), also under the action of D_4 . The $\text{Tree}_{5/3}$ elements generalize the counting of [3 2 1 4] and can be computed in $\mathcal{O}(n^{5/3} \log^2 n)$ time. Among the 10 directions obtained using the marked patterns, two are counted in $\mathcal{O}(n^{5/3} \log^2 n)$ time, by extending the marked pattern [3 2 1 4] to length 5, yielding six double posets under the action of D_4 , while one direction arises from counting occurrences of the pattern [4 3 2 1 5] explicitly in $\mathcal{O}(n^{7/4} \log^2 n)$ time, yielding four double posets under the action of D_4 . As the latter case dominates, the full 5-profile is computable in $\mathcal{O}(n^{7/4} \log^2 n)$ time.
- **6-profile:** Extends the 5-profile with 463 corner trees, 44 tree double posets originating from the family $\text{Tree}_{5/3}$, and 213 *pattern trees* (generalisation of corner trees, introduced in [BL24]), all with six vertices. The 44 tree double posets include elements of $\text{Tree}_{5/3}$ as well as images under nontrivial D_4 actions. The 213 pattern trees can be counted in $\mathcal{O}(n^2 \log^4 n)$ time [BL24], which dominates the computation. Thus, the complete 6-profile is computable in $\mathcal{O}(n^2 \log^4 n)$ time.

3 Experiments

Methodology

Sliding window Instead of computing PE over the entire time series, people often use a *sliding window* approach, which was already proposed in [BP02]. Sliding windows allow for a more localized analysis, often revealing transient changes in the system’s behavior that might be missed when considering the full sequence at once. For that reason, this approach is also useful for GPE, in particular, since GPE considers *all* possible ordinal patterns, the entropy of the *entire* sequence will often be close to 1, independent of the underlying dynamics.

Let k be a fixed order. At each time point t (i.e. using a *stride* of 1; see [LK17] for other choices), we select the window of data points

$$[X_{t-\text{window_size}+1}, \dots, X_t]$$

and compute either $\text{PE}(k; \tau)$, or $\text{GPE}(k)$. Given a time series $(X_t)_{t=1}^n$, this yields a new time series of entropy values $(Y_t)_{t=\text{window_size}}^n$, where each Y_t represents the entropy computed from the window ending at time t . We do emphasize that inside a window, PE considers only consecutive patterns, while GPE considers all patterns.

Choice of window size for GPE The window size should be chosen with an appropriate

sample size in mind. For a reliable estimation of GPE, we need to have a sample size

$$\binom{\text{window_size}}{k} \gg k! \quad (2)$$

much larger than the number of patterns of order k . The window size is varied over a reasonable range, from around the first value satisfying (2) up to half the signal length. In general, a window size that is too small will not capture enough information about the signal, while a window size that is too large will dilute the information by averaging over too many points.

For data which is expected, or known, to have an underlying *periodic structure*, the following approach has proven useful. We compute the entropy values over time by sliding the window along the signal and then averaging these values, obtaining an averaged value of the windowed entropy as a function of the window size. The curve is expected to have a minimum at around half the period of the signal, since in this case the window (sometimes) covers (approximately) increasing or decreasing windows of the signal. If the curve has the shape of a typical curve in Figure 9, the minimum is expected to be near half the period of the signal. In Section 3.3, we observe that selecting a window size between the minimum and twice this value (the expected period) yields good results. Furthermore, in Section 3.2, the best performance for GPE is achieved when the window length is nearly equal to the period.

Choice of window size for PE For PE, the effective sample size is reduced by the delay and order, and is given by

$$\text{window_size} - \tau(k - 1).$$

And again, it needs to be much larger than $k!$. The literature seems to be devoid of a principled approach for selecting the window size. For our experiments, we try several window sizes.

Delay for PE In the literature ([Ban17, Section 4]) it is often recommended to average the delay parameter over a range of values, i.e.,

$$\overline{\text{PE}}(k) := \frac{1}{|\mathcal{T}|} \sum_{\tau \in \mathcal{T}} \text{PE}(k, \tau),$$

where \mathcal{T} is the chosen set of delay values. Additionally, we also consider certain fixed delays.

Order Both entropies depend on the order k . Regarding PE, it is common to try orders in the range of $[3, 7]$ ([BP02]). Regarding GPE, we usually try all currently feasible orders, i.e. $k = 2, 3, 4, 5, 6$.

3.1 Window size and convergence

For a given order k and window length, GPE yields a larger sample size than PE, since the former considers all possible permutation patterns within a window. We generate 100 time series of the form $(X_t)_{t=1}^{50}$, where each X_t is independently drawn from a standard normal distribution. In this fully random setting, the “true” (normalized) values of both PE and GPE are equal to 1. We compare PE and GPE using the same orders $k = 2, 3, 4, 5, 6$. Except for order 2, as the window size n increases, GPE converges to 1 more quickly than PE, see Figure 3.

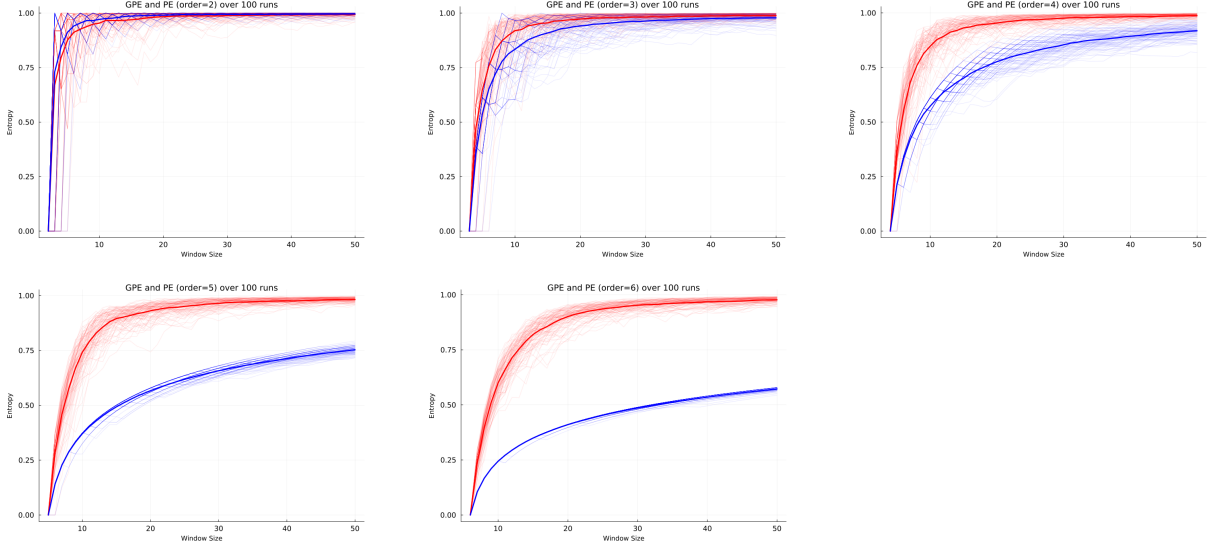


Figure 3: Convergence of GPE (red) and PE (blue) to the value 1 in a fully random sequence.

In order to show that GPE converges faster than PE, we also display the means of the respective 100 realizations of the entropies. Obviously, the convergence becomes slower for higher orders since more patterns need to be counted.

3.2 Noise Detection

We now use PE and GPE to detect an increase in noise within a periodic signal. Fix a period $P \in \{10, 20, 30\}$ and a noise scale parameter $\varepsilon \in \{0.0, 0.25, 0.5, 0.75\}$. The signal $f(t)$ consists of two consecutive segments:

1. **Less Noisy Segment** ($1 \leq t \leq 3P$):

$$f(t) = \sin\left(\frac{2\pi t}{P}\right) + \varepsilon \cdot \eta(t), \quad \eta(t) \sim \mathcal{N}(0, 1),$$

where noise is scaled by ε , resulting in less noise.

2. **More Noisy Segment** ($3P < t \leq \frac{9}{2}P$):

$$f(t) = \sin\left(\frac{2\pi t}{P}\right) + \eta(t), \quad \eta(t) \sim \mathcal{N}(0, 1),$$

where the noise has full variance, representing an increase in noise level.

We then generate 100 independent realizations of such signals and compute entropy values using sliding windows. We compute PE and GPE using orders $k = 2, 3, 4$. We use sliding window sizes that range from 8 to $\frac{3}{2}P + 1$. For PE, for each window size, we evaluate all feasible delay values, where the set of feasible delays is given by

$$\mathcal{T} = \left\{ 1, \dots, \left\lfloor \frac{\text{window_size} - 1}{k - 1} \right\rfloor \right\}.$$

Note that $\left\lfloor \frac{\text{window_size} - 1}{k - 1} \right\rfloor$ represents the largest delay τ that still allows at least one valid k -tuple within the window. For each order k , we also compute the average entropy across feasible delays, $\overline{\text{PE}}(k)$. In our framework, the entropy value (PE or GPE) serves as a classification score

to distinguish less noisy observations from noisier ones. For each Monte Carlo run, we take two equal segments of length $\frac{3}{2}P$: a *less noisy* segment (immediately before the noise onset) and a *more noisy* segment (within the noisier interval). Higher entropy indicates higher noise. Varying a threshold T on entropy, an observation is classified as *more noisy* if $\text{entropy} \geq T$ and *less noisy* otherwise. True/false positives/negatives are defined as usual:

- **TP** = more noisy correctly classified,
- **FN** = more noisy misclassified as less noisy,
- **TN** = less noisy correctly classified,
- **FP** = less noisy misclassified as more noisy.

Sweeping T over all observed entropies yields the ROC curve; the AUC is averaged over 100 Monte Carlo runs with 95% confidence intervals.

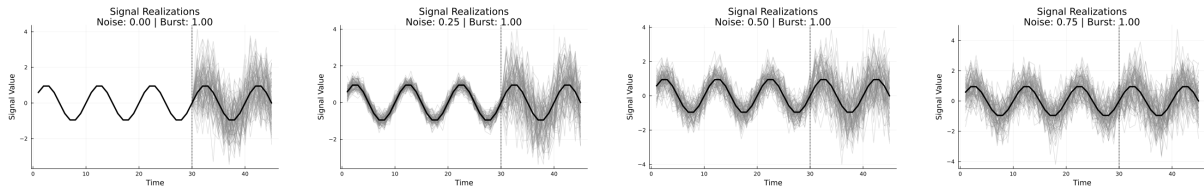


Figure 4: Signal realizations for varying noise levels (ε) with period 10 and length 45.

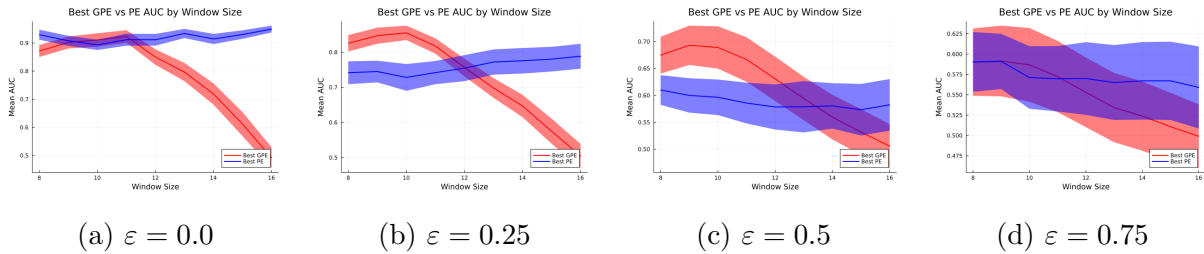


Figure 5: Performance across window sizes (8 to 16) in terms of AUC for noise detection with period 10. For each window size, the highest average AUC among orders $k = 2, 3, 4$ is selected for GPE. For PE, the highest average AUC among orders $k = 2, 3, 4$, feasible delays (or average across delays) is selected.

For $P = 10$, we observe that GPE clearly outperforms PE for noise levels $\varepsilon = 0.25$ and $\varepsilon = 0.5$, see Figure 5. In the absence of noise ($\varepsilon = 0.0$), the performances of PE and GPE are comparable. For the highest noise level ($\varepsilon = 0.75$), both methods perform only slightly better than random classification. Notably, for the cases $P = 20$, and $P = 30$, GPE shows again optimal performance for the window size matching the signal's period (see Figure 6). However, this time, its performance is comparable to that of PE.

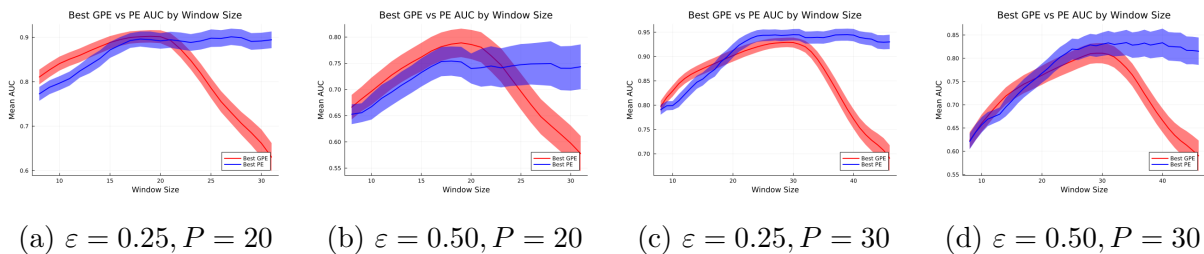
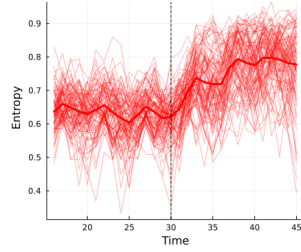
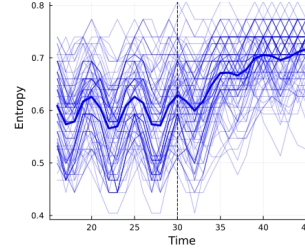


Figure 6: Examples with period 20 and 30



100 realizations of $\text{GPE}(4)$,
 $\text{window_size} = 10$ (average of
curves in thick red)



100 realizations of $\text{PE}(4; 1)$,
 $\text{window_size} = 16$ (average of
curves in thick blue)

Figure 7: Best entropies (yielding the highest average AUC) curves for $P = 10$ and $\varepsilon = 0.25$.
Fifteen observations before the burst and fifteen within the burst.

3.3 Periodic signal with additive noise which increases linearly over time

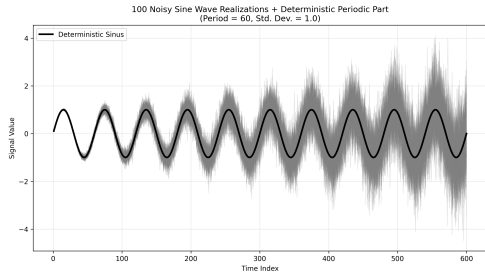


Figure 8: 100 realizations of sinusoidal signal plus modulated noise.

Consider the following signal

$$f(t) = \sin\left(\frac{2\pi t}{P}\right) + \frac{t}{10P} \zeta(t), \quad \zeta(t) \sim \mathcal{N}(0, \sigma^2),$$

where P is the period of the deterministic, periodic component and ζ represents Gaussian white noise with variance $\sigma^2 > 0$, with a prefactor $t/(10P)$ that increases the standard deviation of the noise linearly over time. We consider the signal at time points $t = 1, 2, \dots, 10P$. See Figure 8 for realizations of this signal for $\sigma^2 = 1$, $P = 60$. We expect any measure of entropy to reflect the increasing noise level in the signal, and we compare how GPE and PE behave.

Parameter selection for GPE and PE

For GPE, we use the method described at the beginning of this section to obtain an estimate for (half) the period. As in Figure 9, it usually leads to approximately the correct value of 30. A window size between 30 and 60 is then expected to yield good results.

Regarding PE, as recalled at the beginning of this section, there is no universally agreed methodology for selecting its parameters (window length, delay, etc.). We therefore evaluate PE over multiple window sizes and delays. In addition to computing PE with the default delay of 1, we also evaluate it using delays of 10 and 20. To further reduce sensitivity to any single delay choice, we additionally consider the average over delays in the range 1–10.

Experiment

In Figure 10, we analyze the behavior of both PE and GPE under various signal conditions. The input signals consist of two distinct periods, $P = 60$ and $P = 120$, and are evaluated under two noise levels ($\sigma^2 = 1$ and $\sigma^2 = 4$).

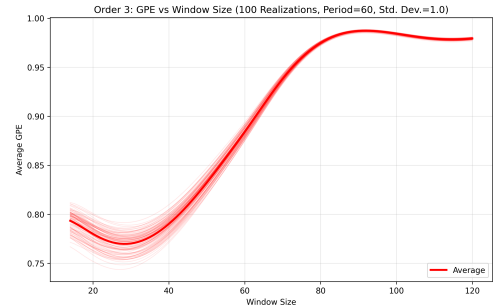


Figure 9: Average sliding-window entropy across different window lengths on signal shown in Figure 8, computed over 100 signal realizations.

We number the plots in Figure 10 left to right, top to bottom.

In Plot 1, for a window size of 30 and $P = 60$, GPE exhibits a highly expressive response, capturing the underlying periodic structure effectively. In contrast, PE with the default delay parameter $\tau = 1$ quickly saturates, thereby losing sensitivity to the signal's structure. We observe generally that PE's performance is significantly affected by the choice of delay. For instance, with delays $\tau = 10$ (Plot 4) and $\tau = 20$ (Plot 2), PE demonstrates erratic behavior with substantial variance across different realizations, indicating a lack of robustness.

Through extensive experimentation and fine-tuning, we found that, for this data, PE achieves the behavior closest to GPE when averaging over delays in the range $\tau = 1$ to $\tau = 10$, specifically for window size 30 and $P = 60$ (as shown in Plot 3). However, this matching behavior degrades as the window size increases. In Plots 5 and 6, corresponding to window sizes 45 and 60 respectively (still with $P = 60$), PE again exhibits early saturation, particularly in Plot 6, whereas GPE remains expressive and continues to reflect the underlying periodicity.

These observations highlight a key advantage of GPE: it is more robust to changes in parameters (e.g., window size) and requires significantly less parameter tuning compared to PE. This robustness is further confirmed in additional experiments (Plot 4 and 5) where we vary the order (e.g., to 4), noise level (e.g., to $\sigma^2 = 4$), period (e.g., to 120), and increase the window size to 150 (different from the ideal window selection of 60 – 120)—under all these conditions, GPE consistently maintains expressive power in representing the signal structure.

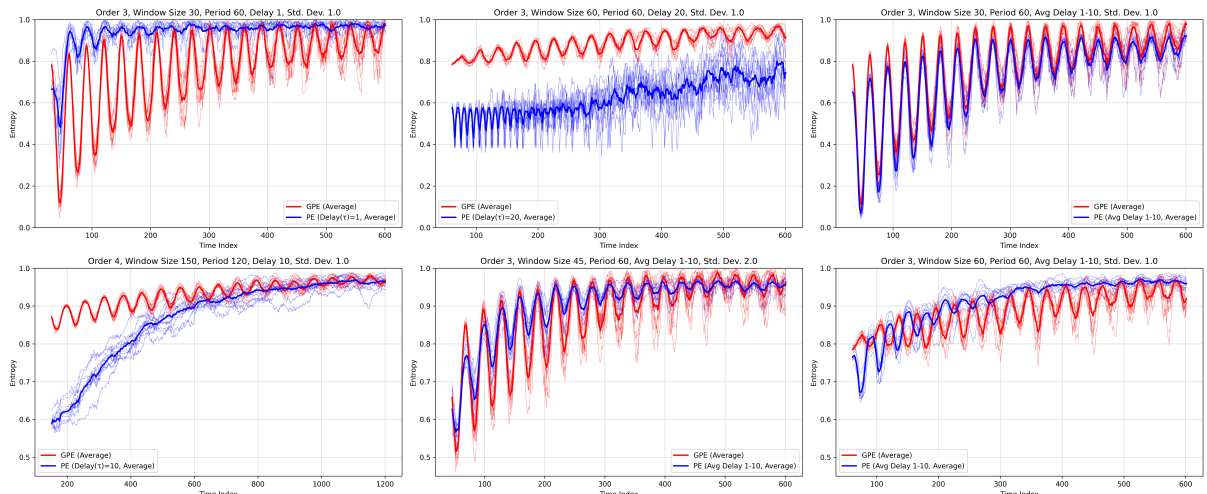


Figure 10: Signal with 100 realizations and average entropy for different window sizes, orders, period of signals, and delays.

4 Conclusion and Outlook

We have introduced Global Permutation Entropy (GPE), a novel complexity measure for time series analysis that extends classical Permutation Entropy by considering all possible ordinal patterns of a given length within a time window, rather than only consecutive or regularly spaced patterns. This conceptually simple extension was previously computationally intractable, but recent algorithmic advances in permutation pattern counting have made its practical implementation feasible for orders up to 6.

The results presented in this paper highlight several desirable features of GPE.

- For completely random signals and fixed order $k > 2$, $\text{GPE}(k)$ converges faster than $\text{PE}(k)$ to the expected value of 1. This is because GPE utilizes *all possible ordinal patterns* within

the window, effectively increasing the sample size for the same window length compared to PE, which only considers a tiny subset of patterns. See Section 3.1.

- In certain settings, GPE also detects changes in noisy periodic signals more quickly than PE, when there is a sudden increase in noise level. We observed this for short signals, where PE struggles due to insufficient sample size. See Section 3.2.
- When gradually adding noise to a periodic signal, GPE remains highly descriptive and robust across different orders and window sizes. Notably, GPE performs well when the window size is chosen between half the period and one full period. This characteristic makes GPE simpler and easier to use than PE, which requires careful tuning of delay parameters or averaging over multiple delays to achieve comparable performance. See Section 3.3.

The larger effective sample size of GPE compared to PE leads to at least two consequences: the granularity of the entropy values is finer (since the “step size” in (1) is $\binom{\text{window_size}}{k}$ instead of $\text{window_size} - k + 1$), and entropy values are generally higher than for PE (see Figure 7). Indeed, in our experiments, we observe that the value of GPE is often close to 1 but evolves on a finer scale than PE. Furthermore, when sliding the window from time step t to $t + 1$, at most one histogram element changes for PE, but up to $\binom{\text{window_size} - 1}{k - 1}$ elements may change for GPE. For PE, the relative change in the histogram is either zero or exactly $\frac{1}{\text{window_size}}$. In contrast, for GPE, changes can take values from $\left\{0, \frac{1}{\binom{\text{window_size}}{k}}, \dots, \frac{k}{n}\right\}$, since $\frac{\binom{\text{window_size} - 1}{k - 1}}{\binom{\text{window_size}}{k}} = \frac{k}{n}$. It would be interesting to explore whether the finer granularity and more dynamic behavior of GPE could be leveraged to achieve a good performance in certain settings.

Furthermore, future work could also include:

- Identifying real data sets for which GPE performs better than PE.
- Providing a fast implementation of profile 7 and therefore of GPE(7). This is already feasible, relying on results from [BL24].
- Permutation entropy considers only consecutive or regularly spaced patterns. Global permutation entropy considers all patterns (also known as the classical permutation patterns). What other types of patterns could be considered to define a permutation entropy?
- Consider a measure of entropy based on corner trees as follows. For a fixed order k , consider the maximal set of corner trees with k vertices that span linearly independent directions of patterns. Let $\{T_1, \dots, T_m\}$ denote these trees, and let c_i be the number of occurrences of T_i in the ranked time series, with total $C = \sum_{i=1}^m c_i$. Define the empirical distribution $p_i = c_i/C$. The raw *corner-tree entropy* is given by

$$\widehat{\text{CTPE}}(k) := - \sum_{i=1}^m p_i \log p_i.$$

Note that, although from level 4 onward the corner trees no longer span the entire profile, this entropy can be evaluated in just $\mathcal{O}(n \log n)$ time.

- Applying known extensions of PE to GPE, such as conditional entropy [UK14].

References

[Avh+25] Abhijeet Avhale et al. *Global Permutation Entropy*. <https://github.com/AThreeH1/globalpermutationentropy>. GitHub repository. 2025.

[Ban17] Christoph Bandt. “A new kind of permutation entropy used to classify sleep stages from invisible EEG microstructure”. In: *Entropy* 19.5 (2017), p. 197.

- [BL24] Gal Beniamini and Nir Lavee. “Counting Permutation Patterns with Multidimensional Trees”. In: *arXiv preprint arXiv:2407.04971* (2024).
- [BP02] Christoph Bandt and Bernd Pompe. “Permutation entropy: a natural complexity measure for time series”. In: *Physical review letters* 88.17 (2002), p. 174102.
- [DV24] Joscha Diehl and Emanuele Verri. “Efficient counting of permutation patterns via double posets”. In: *arXiv preprint arXiv:2408.08293* (2024).
- [EL21] Chaim Even-Zohar and Calvin Leng. “Counting small permutation patterns”. In: *Proceedings of the 2021 ACM-SIAM Symposium on Discrete Algorithms (SODA)*. SIAM. 2021, pp. 2288–2302.
- [Fer+14] Edoardo Ferlazzo et al. “Permutation entropy of scalp EEG: A tool to investigate epilepsies: Suggestions from absence epilepsies”. In: *Clinical Neurophysiology* 125.1 (2014), pp. 13–20.
- [KL03] Karsten Keller and Heinz Lauffer. “Symbolic analysis of high-dimensional time series”. In: *International Journal of Bifurcation and Chaos* 13.09 (2003), pp. 2657–2668.
- [Liu+22] Minhao Liu et al. “Scinet: Time series modeling and forecasting with sample convolution and interaction”. In: *Advances in Neural Information Processing Systems* 35 (2022), pp. 5816–5828.
- [LK17] Douglas J Little and Deb M Kane. “Variance of permutation entropy and the influence of ordinal pattern selection”. In: *Physical Review E* 95.5 (2017), p. 052126.
- [LOR07] Xiaoli Li, Gaoxian Ouyang, and Douglas A Richards. “Predictability analysis of absence seizures with permutation entropy”. In: *Epilepsy research* 77.1 (2007), pp. 70–74.
- [UK14] Anton M Unakafov and Karsten Keller. “Conditional entropy of ordinal patterns”. In: *Physica D: Nonlinear Phenomena* 269 (2014), pp. 94–102.
- [ZSW13] Xiaojun Zhao, Pengjian Shang, and Jing Wang. “Measuring information interactions on the ordinal pattern of stock time series”. In: *Physical Review E—Statistical, Nonlinear, and Soft Matter Physics* 87.2 (2013), p. 022805.